LETTER Communicated by Bard Ermentrout

Analytic Expressions for Rate and CV of a Type I Neuron Driven by White Gaussian Noise

Benjamin Lindner
Lindner.Benjamin@science.uottawa.ca
André Longtin
alongtin@physics.uottawa.ca
Department of Physics, University of Ottawa, Ottawa, Canada KIN 6N5

Adi Bulsara
bulsara@spawar.navy.mil
SPAWAR Systems Center, San Diego, CA 92152-6147, U.S.A.

We study the one-dimensional normal form of a saddle-node system under the influence of additive gaussian white noise and a static "bias current" input parameter, a model that can be looked upon as the simplest version of a type I neuron with stochastic input. This is in contrast with the numerous studies devoted to the noise-driven leaky integrate-and-fire neuron. We focus on the firing rate and coefficient of variation (CV) of the interspike interval density, for which scaling relations with respect to the input parameter and noise intensity are derived. Quadrature formulas for rate and CV are numerically evaluated and compared to numerical simulations of the system and to various approximation formulas obtained in different limiting cases of the model. We also show that caution must be used to extend these results to the Θ neuron model with multiplicative gaussian white noise. The correspondence between the first passage time statistics for the saddle-node model and the Θ neuron model is obtained only in the Stratonovich interpretation of the stochastic Θ neuron model, while previous results have focused only on the Ito interpretation. The correct Stratonovich interpretation yields CVs that are still relatively high, although smaller than in the Ito interpretation; it also produces certain qualitative differences, especially at larger noise intensities. Our analysis provides useful relations for assessing the distance to threshold and the level of synaptic noise in real type I neurons from their firing statistics. We also briefly discuss the effect of finite boundaries (finite values of threshold and reset) on the firing statistics.

1 Introduction

The transition from quiescent to periodic firing behavior as a bias current increases leads to significant changes in the dynamics of an excitable

system. This transition is characterized by the behavior of the firing frequency across this transition. It is possible to divide neurons according to this behavior into type I and type II dynamics (Hodgkin, 1948). Type I dynamics exhibit a continuous variation in firing frequency as a bias parameter (such as an input current) is increased. Dynamically, such a transition to repetitive firing is associated with a saddle-node bifurcation (Rinzel & Ermentrout, 1989). At this bifurcation, a stable and an unstable fixed point coalesce and disappear, with a stable limit cycle taking their place. In the neural modeling context, the stable fixed point is associated with the resting potential, while the unstable fixed point (and associated unstable direction(s) or "unstable manifold" in phase space) is associated with the threshold of the cell. Type II membranes exhibit a finite nonzero frequency as repetitive firing begins. Such transitions are associated with Hopf bifurcations. Some model and experimental systems can exhibit transitions to repetitive firing by one or the other of these mechanisms, depending on system parameters.

The relevance of noise-induced firing in type I membranes is related to the problem of large coefficients of variation (CVs). There has been much effort to explain the observed variability in firing rates in various experimental preparations, and much attention has been devoted to the occurrence of interspike interval histograms (ISIH) with high CVs defined as the ratio of ISIH standard deviation to mean (Wilbur & Rinzel, 1983; Softky & Koch, 1993; Shadlen & Newsome, 1994; Bell, Mainen, Tsodyks, & Sejnowski, 1995; Troyer & Miller, 1997). Gutkin and Ermentrout (1998) have shown using numerical simulations that large CVs can be obtained from type I dynamics with noise. They used the so-called one-dimensional Θ neuron model (Ermentrout, 1996) and compared results from stochastic simulations of this model with those from simulations of the two-dimensional Morris-Lecar model (Morris & Lecar, 1981; Rinzel & Ermentrout, 1989) that has inspired the elaboration of the Θ neuron model. Other researchers (Gang, Ditzinger, Ning, & Haken, 1993; Rappel & Strogatz, 1994) have also explored the effect of noise on saddle-node bifurcations in a generic dynamical system, while Longtin (1997) has studied the effect of noise on this bifurcation in the Hindmarsh-Rose bursting neuron model and shown how the ISIHs and other firing statistics vary with noise strength.

The origin of the high variability seen in certain experiments and in noise-driven models of type I membranes can be understood from the seminal theoretical work of Sigeti and Horsthemke (1989). They studied how noise can move the state variable across the unstable fixed point associated with a saddle-node bifurcation. Their analysis was performed on a one-dimensional dynamical system known as the normal form of the saddle-node bifurcation. This system describes the long-lived dynamics of a (possibly higher-dimensional) system in the vicinity of this bifurcation, all other aspects of the dynamics having decayed away to zero. More precisely, their

analysis was confined to the bifurcation point itself, where the saddle and the node have coalesced into a semistable fixed point. In other words, they focused on the normal form $\dot{x} = \beta + x^2$ with $\beta = 0$; they also considered the Adler equation $\dot{\theta} = 1 - \cos\theta$, a variant of this normal form, which agrees with it to second order. In neural terms, that means that the bias current is set right at rheobase.

The analysis of Sigeti and Horsthemke (1989) described how noise pushes solutions over the saddle-node point in terms of the two first moments of the first passage time density. While those theoretical and computational studies were carried out at the bifurcation, our study aims to explore the vicinity of this bifurcation, thus making it relevant to a range of experimentally plausible parameters in real neurons. The goal of our article is to provide analytical insight into how noise, for example, of synaptic origin, affects the transition to repetitive firing in type I membranes. We give exact and simplified approximate expressions for the mean interspike interval (ISI), the ISI standard deviation, and CV defined as the ratio of standard deviation to mean; these expressions are sought as a function of the input parameters.

The article is organized as follows. In section 2.2, we introduce our basic spike generator model, discuss its relation to the Θ neuron, and derive some scaling relations for rate and CV with respect to the input parameters. In section 3, we give exact integral expressions for the first two central moments of the interspike interval and derive simple approximations for various limit cases. The results, rate and CV as functions of constant input and noise intensity, are presented in section 4. Here we also compare results from two different versions of the stochastic Θ model and those from our basic model; furthermore, we discuss briefly how the firing statistics change for finite boundaries in the associated passage time problem. In section 5, our results are summarized and briefly discussed in a more general context. Two appendixes contain supplementary material.

2 The Model and Its Basic Properties

2.1 Stochastic Spike Generator Model for a Type I Neuron. Every system that is close to a saddle-node bifurcation will be dominated by the quasi-one-dimensional passage through the region around its fixed point. This holds true also for many neurons known as type I neurons and in particular for neuron models like, for instance, the Morris-Lecar model (Morris & Lecar, 1981). The influence of noise on such a system is of eminent importance for issues like spike train variability and reliability of signal transmission through neurons. Moreover, the typical spike train input received by many higher-order neurons can be also approximated by a simple noise process (diffusion approximation; see, for instance, Tuckwell, 1988). The simplest choice for a random input that still permits an extensive analytical

treatment is an uncorrelated noise—a white noise.[1] We allow for a finite mean value of the noise that can be looked upon as a separate constant input.

After the usual reduction procedure from the multidimensional dynamics (Ermentrout, 1996; Gutkin & Ermentrout, 1998; Hoppensteadt & Izhikevich, 1997), the one-dimensional normal form driven by a white noise input reads

$$\dot{x} = \beta + x^2 + \sqrt{2D}\xi(t). \tag{2.1}$$

Here, time is measured in the typical timescale of the model. The parameter D denotes the noise intensity, and the gaussian white noise $\xi(t)$ obeys the correlation function $\langle \xi(t)\xi(t+\tau)\rangle = \delta(\tau)$. The parameter β is another input parameter; it is constant and can also be thought of as a static or very slowly varying signal. We note that this reduction has assumed a prior approximation regarding the nature of the noise. If the noise is meant as synaptic input to a cell, this input modifies the conductances that multiply the usual "battery" terms $(V_{rev} - V)$ in the Hodgkin-Huxley formalism. This gives rise to multiplicative noise, since the state variable (the voltage) multiplies the noise (the fluctuating conductance). The reduction is assumed to take place very near the bifurcation, so that the noise can be made additive (the voltage is set to a constant in the synaptic battery terms). It is not known generally what effect this approximation has on the dynamics, except right near the bifurcation.

We consider in this work a simple spike generator that produces spikes whenever the variable x reaches a threshold value x_+. After occurrence of a spike, the variable is reset to a negative value x_-. If not stated otherwise, these values are chosen to be at plus and minus infinity, respectively. A version of this spike generator with finite threshold and reset values (although possibly with a different kind of input current) is known as the quadratic integrate-and-fire neuron and has been recently used in studies of neuronal networks (see, e.g., Latham, Richmond, Nelson, & Nirenberg, 2000; Hansel & Mato, 2001); here, we discuss the effect of finiteness of $x_\pm$ briefly (see section 4.4). The ISIs are obtained from independent realizations of the passage from x_- to x_+. The presence of the square term and the white gaussian noise in equation 2.1 ensures that this passage time is finite (in spite of the possibly infinite threshold and reset values) for all values of the input parameter β.

A simulation of the system can be performed for only finite initial and threshold points x_- and x_+, respectively. Starting at $x_0 = x_-$, the dynamics equation 2.1 can be numerically integrated with a sufficiently small time

[1] The term *white* refers to the power spectrum of the noise, which is flat, that is, contains all frequency (as white light contains all frequencies of the visible electromagnetic spectrum). A flat spectrum in turn implies a δ correlation of the noise (Risken, 1984). The process has no correlations over a finite time at all.

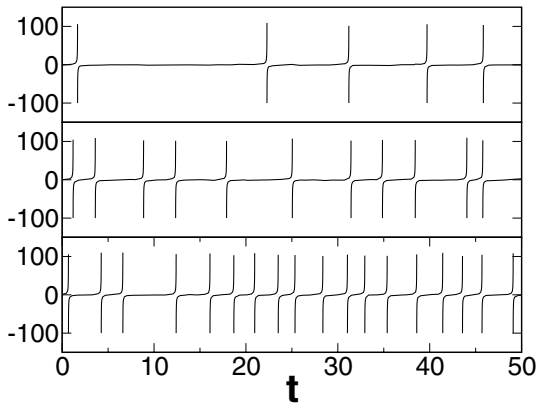

Figure 1: Trajectories of the model obtained by a simulation of the stochastic differential equation, 2.2, with threshold and reset parameters $x_\pm = \pm 100$, $D = 1$, $\Delta t = 10^{-3}$, and $\beta = -1, 0, 1$ (from top to bottom).

step Δt,

$$x_{j+1} = x_j + (\beta + x_j^2)\Delta t + \sqrt{2D\Delta t}\,\xi_j, \tag{2.2}$$

where $x_j \doteq x(j\Delta t)$ and the ξ_j is a sequence of independent gaussian random numbers with unit variance (Risken, 1984). The rule for reset and generation of the ith firing time t_i is

$$x(t) = x_+ \to t_i \doteq t \text{ and } x(t^+) = x_-. \tag{2.3}$$

The firing (spike) times are defined as the instants at which x crosses x_+; the variable x is reset to x_- right after occurrence of a spike. The points x_- and x_+ should be chosen sufficiently large and the time step sufficiently small such that a further increase or decrease, respectively, does not change the statistics of the measured quantities of interest significantly (as mentioned, the effect of finite $x_\pm$ is studied in section 4.4). Three example trajectories for different values of β are shown in Figure 1. The sequence of firing times generated by the model $(\ldots, t_{i-1}, t_i, t_{i+1}, \ldots)$ describes a renewal point process (Cox, 1962); subsequent intervals between firing times, $T_i = t_i - t_{i-1}$ and $T_{i+1} = t_{i+1} - t_i$, are statistically independent (therefore, we omit in the following the index i). Here, we study two basic quantities: the stationary firing rate and the CV.

The stationary firing rate is given by the inverse of the mean interspike interval $\langle T \rangle$ (with the brackets standing for an ensemble average):

$$r(\beta, D) = \frac{1}{\langle T \rangle}. \tag{2.4}$$

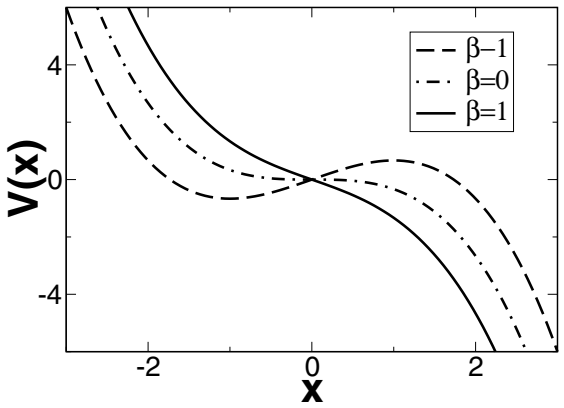

Figure 2: Potential associated with equation 2.1 for different values of β.

The CV is the relative standard deviation of the interspike interval; it is a second-order quantity that measures the variability of spiking and is given by

$$CV(\beta, D) = \frac{\sqrt{\langle \Delta T^2 \rangle}}{\langle T \rangle}, \tag{2.5}$$

where $\langle \Delta T^2 \rangle = \langle T^2 - \langle T \rangle^2 \rangle$ stands for the variance.

Before we proceed, we give an instructive mechanical analogy for the dynamics equation 2.1. We may associate a potential with equation 2.1, the derivative of which yields the deterministic part of the right-hand side (the constant of integration has been chosen to be zero):

$$V(x) = -x^3/3 - \beta x. \tag{2.6}$$

Depending on the value of β, this potential exhibits for $\beta < 0$ a minimum and a maximum, for $\beta = 0$ a saddle point, or for $\beta > 0$ no extrema at all, resulting in quite different statistics of the passage times and thus of the spike train. In Figure 2, we show these different shapes that correspond to the following firing regimes of the type I neuron: $\beta < 0$ noise-activated firing, that is, the ISI is dominated by the noise-assisted escape from the potential minimum at $x = -\sqrt{\beta}$ over the potential barrier at $x = \sqrt{\beta}$, corresponding to the famous Kramers problem (Kramers, 1940); $\beta = 0$ right at the saddle-node bifurcation, where no firing occurs without noise but the statistics of interspike intervals (first passage time of particle) is very particular (Sigeti & Horsthemke, 1989); and $\beta > 0$ the oscillatory ("running") regime, where the associated potential has no minimum ("downhill motion").

2.2 Relation to the Θ Neuron Model. The dynamics equation 2.1 can be transformed to the so-called Θ neuron model by the new variable (Ermentrout, 1996),

$$\Theta = 2\arctan(x), \tag{2.7}$$

resulting in a stochastic differential equation with multiplicative white noise (i.e., the prefactor of the noise term depends on the state variable),

$$\dot{\Theta} = (1 - \cos(\Theta)) + (1 + \cos(\Theta))(\beta + \sqrt{2D}\xi(t)). \tag{2.8}$$

For this phase oscillator model, threshold and reset values are at finite values—at $-\pi$ and π, respectively. The Θ model with a white noise input current, however, must be treated with caution. A stochastic differential equation with multiplicative noise is not uniquely determined; it has to be supplemented by an interpretation (so-called Ito-Stratonovich dilemma; see Gardiner, 1985). This seems to be paradoxical since the original dynamics equation 2.1, which is driven by additive noise, is nonambiguous. The resolution of this paradox is given by the fact that the Stratonovich interpretation is the only interpretation that permits the usual transformation of variables (Gardiner, 1985). Since equation 2.8 results from such a transformation (namely, equation 2.7), we have to interpret equation 2.8 in Stratonovich's sense. This is also plausible for another reason: driving currents in real neurons are never white noise but will have a finite correlation time; white noise that is thought of as the limit of a "colored" noise with negligible correlation time leads to the Stratonovich interpretation of a dynamics with multiplicative noise (see, e.g., Risken, 1984).

In the following, we wish to use a simple Euler integration algorithm (see, e.g., Risken, 1984), which assumes the Ito interpretation. Thus, we must first express our Stratonovich stochastic differential equation into its corresponding Ito form. This correspondence preserves the physics of the problem. This Ito equivalent stochastic differential equation, 2.8, has an additional drift term $-D\sin(\Theta)(1+\cos(\Theta))$. The integration scheme analog to equation 2.2 then reads

$$\begin{aligned}\Theta_{j+1} = \Theta_j &+ [(1 - \cos\Theta_j) + (\beta - D\sin\Theta_j)(1 + \cos\Theta_j)]\Delta t \\ &+ \sqrt{2D\Delta t}(1 + \cos\Theta_j)\xi_j,\end{aligned} \tag{2.9}$$

where ξ_j is again a sequence of independent gaussian distributed random numbers with unit variance. Note that in Gutkin and Ermentrout (1998), the drift term is apparently missing, and hence the dynamics has been interpreted in the sense of Ito. This leads to the following integration scheme,

$$\begin{aligned}\Theta_{j+1} = \Theta_j &+ [(1 - \cos\Theta_j) + \beta(1 + \cos\Theta_j)]\Delta t \\ &+ \sqrt{2D\Delta t}(1 + \cos\Theta_j)\xi_j,\end{aligned} \tag{2.10}$$

which is also the one that could be expected from a straightforward (although inexact) inclusion of gaussian white noise in the Θ neuron dynamics.

Clearly, the difference between equations 2.10 and 2.9 vanishes in the weak noise limit since the additional Stratonovich drift in equation 2.9 is proportional to noise intensity D. We will show that simulation of the Stratonovich version indeed yields the same statistics of interspike intervals as the original dynamics equation, 2.1, whereas the Ito interpretation, equation 2.10 of the Θ neuron model, which was used by Gutkin and Ermentrout (1998), leads to different results in particular at moderate to large noise intensity.

2.3 Scaling Relations. We return now to the original model, equation 2.1. Therein, we have two free parameters, β and D. If we properly rescale x and t, it is possible to obtain the same nonlinearities as in equation 2.1, except for a new combination of the parameters β and D (threshold and reset values do not change in any case since they remain at plus and minus infinity, respectively). This gives us scaling relations for rate and CV with respect to the input parameters D and β. Moreover, we can eliminate one of the parameters, although we still have to distinguish among the three different firing regimes. For $\beta = 0$, which has been treated by Sigeti (1988), that is, for

$$\dot{x} = x^2 + \sqrt{2D}\xi(t), \tag{2.11}$$

we choose the new variable and time as

$$y = x/a, \quad \tilde{t} = at \tag{2.12}$$

with a arbitrary but positive. This leads to[2]

$$\dot{y} = y^2 + \sqrt{2D/a^3}\xi(\tilde{t}). \tag{2.13}$$

With $a = D^{1/3}$ we can eliminate the noise intensity (Sigeti, 1988). Of course, the moments of ISI will be still rescaled according to equation 2.12; however, the CV, which is the relative standard deviation of the ISI, remains the same for all values of D:

$$\begin{aligned} &CV(\beta = 0, D) = CV(\beta = 0, D/a^3) \\ &\quad \Rightarrow CV(\beta = 0, D_1) = CV(\beta = 0, D_2). \end{aligned} \tag{2.14}$$

[2] Note that $\xi(t/a) = \sqrt{a}\xi(t)$, which can be seen by considering the correlation function: $\langle \xi(t/a)\xi(t'/a)\rangle = \delta([t - t']/a) = a\delta(t - t') = \langle \sqrt{a}\xi(t)\sqrt{a}\xi(t')\rangle$.

The elimination of noise intensity is also possible for $\beta \neq 0$. (This fact was also suggested independently by E. Izhikevich, personal communication.) With respect to the approximations we shall derive, it is, however, more convenient to set $a = \sqrt{|\beta|}$. This yields the following dynamics:

$$\begin{aligned}\dot{y} &= \frac{\beta}{|\beta|} + y^2 + \sqrt{2D/|\beta|^{3/2}}\xi(\tilde{t}) \\ &= \begin{cases} +1 + y^2 + \sqrt{2D/|\beta|^{3/2}}\xi(\tilde{t}), & \beta > 0 \\ -1 + y^2 + \sqrt{2D/|\beta|^{3/2}}\xi(\tilde{t}), & \beta < 0 \end{cases}. \end{aligned} \tag{2.15}$$

We obtain the same dynamics with rescaled noise intensity and an input that is either plus or minus one. Thus, to understand the dynamics of the model, it suffices to consider the three cases where $\beta = \pm 1$ or 0.

Obviously, the new timescale rescales also the moments of the passage time by $\langle \tilde{T}^n \rangle = |\beta|^{\frac{n}{2}} \langle T^n \rangle$. Using this and the above relations, we find the following scaling relations for rate and CV ($\beta \neq 0$),

$$r(\beta, D) = \sqrt{|\beta|} r(\pm 1, |\beta|^{-3/2} D) \tag{2.16}$$

$$\langle \Delta T^2 \rangle(\beta, D) = |\beta|^{-1} \langle \Delta T^2 \rangle(\pm 1, |\beta|^{-3/2} D) \tag{2.17}$$

$$CV(\beta, D) = CV(\pm 1, |\beta|^{-3/2} D), \tag{2.18}$$

where the sign on the right-hand side coincides with that of β.

From the first equation, it can be inferred that for positive input ($\beta > 0$) and vanishing noise, the rate scales like $r \sim \sqrt{\beta}$. In the presence of noise, an increase in β diminishes the effective noise intensity.

The third equation is even more important. The range of possible CVs does not depend on β as long as its sign is fixed. Plotting the CV as a function of noise intensity results always in the same curve apart from a stretching by $|\beta|^{-3/2}$ in the argument. Furthermore, we see from equation 2.18 that the CV in the large noise limit corresponds to the CV at finite D but vanishing input,

$$\begin{aligned}\lim_{D\to\infty} CV(\beta, D) &= \lim_{D\to\infty} CV(\pm 1, |\beta|^{-3/2} D) \\ &= \lim_{\beta\to 0} CV(\pm 1, |\beta|^{-3/2} D) = CV(0, D). \end{aligned} \tag{2.19}$$

By similar arguments, asymptotic scaling relations for strong noise (or equivalently weak input β) can be derived, given by

$$r(\pm 1, D) \approx A_1 D^{1/3} + B_1 \beta D^{-1/3}, \quad D \to \infty \tag{2.20}$$

$$CV(\pm 1, D) \approx A_2 + B_2 \beta D^{-2/3}, \quad D \to \infty. \tag{2.21}$$

In these formulas A_1, A_2, B_1, and B_2 denote numerical constants, which will be given below. Small noise intensity will require higher-order terms in β (rate and CV in equations 2.20 and 2.21 diverge for $D \to 0$, which is not expected from the biological point of view) and thus the linearity with respect to input depends strongly on the noise level.

3 Exact and Approximate Expressions for Spike Rate and CV

3.1 Exact Formulas for the First Two Central Moments of the Interspike Interval Distribution. The hierarchy of quadrature expressions for the moments of the passage time problem in an arbitrary potential have been known for a long time (Pontryagin, Andronov, & Witt, 1989). The standard expressions for mean and variance of the first passage time can be somewhat simplified (see appendix A), yielding

$$\langle T \rangle = \left(\frac{9}{D}\right)^{1/3} \int_{-\infty}^{\infty} dx\, e^{-\alpha x - x^3} \int_{-\infty}^{x} dy\, e^{\alpha y + y^3} \tag{3.1}$$

$$\langle \Delta T^2 \rangle = \left(\frac{9}{D}\right)^{2/3} \int_{-\infty}^{\infty} dx\, e^{-\alpha x - x^3} \int_{x}^{\infty} dy\, e^{-\alpha y - y^3} \left[\int_{-\infty}^{x} dz\, e^{\alpha z + z^3}\right]^2 \tag{3.2}$$

$$\alpha = \left(\frac{3}{D^2}\right)^{1/3} \beta.$$

These formulas correspond to infinite threshold and reset values $x_\pm = \pm\infty$. The quadratures for the case of finite reset and finite threshold values are given in the appendix by equations A.1 and A.4. The integrals in equations 3.1 and 3.2 may be evaluated numerically by standard procedures.[3] There are, however, a number of cases where the integrals can be carried out analytically, which gives us some additional control over the accuracy of our numerical integration.

First, the mean first passage time (i.e., the mean ISI) can be expressed by an infinite sum (Colet, San Miguel, Casademunt, & Sancho, 1989) as follows:[4]

$$\langle T \rangle = \left(\frac{1}{3D}\right)^{1/3} \sqrt{\frac{\pi}{3}} \sum_{n=0}^{\infty} (-1)^n \frac{2^{(2n+1)/3}}{n!} \Gamma\left(\frac{2n+1}{6}\right) \left(\beta \sqrt[3]{\frac{3}{D^2}}\right)^n. \tag{3.3}$$

[3] The infinite integration boundaries have to replaced by finite ones that are chosen sufficiently large such that a further increase does not change the results to within the desired accuracy.

[4] Note that there are write errors in equations 3.6 and 3.7 of Colet et al. (1989).

Here $\Gamma(\cdot)$ denotes the gamma function (Abramowitz & Stegun, 1970). This formula is especially useful for large noise intensities, whereas in the weak noise limit, many terms are required to achieve convergence.

Furthermore, for $\beta = 0$ both mean and variance of the ISI can be calculated analytically (see Sigeti, 1988; Sigeti & Horsthemke, 1989). The result is simple and reads

$$\langle T(\beta = 0)\rangle = [\Gamma(1/3)]^2 \left(\frac{1}{3D}\right)^{1/3}. \tag{3.4}$$

$$\langle \Delta T^2(\beta = 0)\rangle = \frac{1}{3}[\Gamma(1/3)]^4 \left(\frac{1}{3D}\right)^{2/3} = \frac{1}{3}\langle T\rangle^2. \tag{3.5}$$

The latter equality in equation 3.5 implies that for $\beta = 0$, the ratio of variance and mean square of the ISI (and hence also the CV) is a constant and independent of noise intensity in accordance with equation 2.14. Rate and CV of the type I neuron read in this case

$$r(\beta = 0, D) = \frac{1}{[\Gamma(1/3)]^2}(3D)^{1/3} \approx 0.201 D^{1/3},$$
$$CV(\beta = 0, D) = 1/\sqrt{3}. \tag{3.6}$$

Since the integral and sum formulas above are not very transparent, we shall derive some simplifications that apply in different limit cases: (1) weak noise and positive input ($\beta > 0$, oscillatory regime), that is, limit cycle dynamics weakly perturbed by noise; (2) weak noise and negative input ($\beta < 0$, excitable regime), that is, excitations are rare and an escape rate description applies; and (3) weak input or strong noise limit.

3.2 Rate and CV in the Oscillatory Regime at Weak Noise. For a strictly monotonously decreasing potential (as in our problem for $\beta > 0$), general approximation formulas for the mean and the variance of the passage time to linear order in D were given by Arecchi and Politi (1980) and yield in our case

$$\langle T\rangle \approx \pi/\sqrt{\beta}, \tag{3.7}$$

$$\langle \Delta T^2\rangle \approx \frac{3D\pi}{4\beta^{5/2}}. \tag{3.8}$$

There is no linear contribution in D to the mean ISI; the value $\pi/\sqrt{\beta}$ is clearly the deterministic passage time along the entire x-axis. Both this time and the variance of the passage time decrease with increasing β.

For rate and CV, we find

$$r \approx \sqrt{\beta}/\pi, \qquad CV = \sqrt{\frac{3D}{4\pi}}\beta^{-3/4} \quad \text{for} \quad \beta \gg D^{2/3}. \tag{3.9}$$

This scaling behavior (independence of mean ISI of D, variance of ISI going as $\sqrt{D}$) resembles that of a perfect integrate-and-fire (PIF) neuron driven by white noise (see, e.g. Bulsara, Lowen, & Rees, 1994). Indeed, for weak noise and positive input, one may even approximate the ISI probability density function (PDF) by an inverse gaussian (i.e., the ISI PDF for a perfect integrate-and-fire neuron)—an approach that works rather well and will be presented elsewhere.

3.3 Rate in the Excitable Regime and Weak Noise. For $\beta < 0$ and weak noise, the passage from minus to plus infinity is dominated by the escape from the potential minimum at $x_- = -\sqrt{\beta}$ over the barrier at $x_+ = \sqrt{\beta}$. A standard saddle-point approximation of the integral in equation 3.1 yields an exponential firing rate (Colet et al., 1989),

$$r = \frac{\sqrt{|\beta|}}{\pi} \exp\left[-\frac{4|\beta|^{3/2}}{3D}\right] \quad \text{for} \quad D \ll |\beta|^{3/2}, \tag{3.10}$$

which is the Kramers escape rate for the potential equation 2.6 in the overdamped case (Kramers, 1940). A similar approximation of the variance in equation 3.2 gives the square of the mean ISI; such an approach yields a CV of unity equivalent to the rare-event statistics of a Poisson process.

3.4 Rate and CV in the Case of Weak Input or Strong Noise. If the input β is weak in amplitude or, equivalently, the noise intensity is sufficiently strong ($|\beta| \ll D^{2/3}$), we expect that rate and CV deviate only linearly from the simple expressions in equation 3.6.

To find this linear expansion for the firing rate, we keep only the first two terms in the sum formula of the mean ISI, equation 3.3, and expand the rate with respect to β. This yields, after some manipulations,

$$\begin{aligned} r(\beta \ll 1, D) &\approx \frac{(3D)^{1/3}}{[\Gamma(1/3)]^2} + \frac{9}{8}\frac{3^{1/6}}{\pi^3}[\Gamma(2/3)]^4 D^{-1/3}\beta \\ &\approx 0.201\, D^{1/3} + 0.147 D^{-1/3}\beta. \end{aligned} \tag{3.11}$$

For the CV, the numerical constant, namely, the derivative of the CV with respect to β, can be performed only numerically. We find that this derivative is well approximated by $1/4D^{-2/3}$,

$$\begin{aligned} CV(\beta \ll 1, D) &\approx \frac{1}{\sqrt{3}} + \frac{1}{4} D^{-2/3}\beta \\ &\approx 0.578 + 0.250 \cdot D^{-2/3}\beta. \end{aligned} \tag{3.12}$$

Clearly, equations 3.11 and 3.12 can be not only used in case of a weak input but also regarded as large noise asymptotic.

4 Results

In the next two sections, we discuss rate and CV as functions of the noise intensity and the constant input. In all figures, lines for $\beta \neq 0$ were obtained by numerical evaluation of the quadrature formulas, 3.1 and 3.2,[5] and insertion into equations 2.4 and 2.5; for $\beta = 0$ formula equation 3.6 was used. Symbols indicate results of numerical simulations of the dynamics using reset and absorption points $x_\pm = \pm 500$, a Euler scheme with $\Delta t = 10^{-3}$ or $\Delta t = 10^{-4}$ (the latter at large noise intensity). Depending on parameters, up to 10^5 spikes were used for estimation of the statistics of the interspike interval. In the upper panels of all figures, we compare the numerically evaluated quadrature results and the numerical simulations. They are in all cases in excellent agreement with each other, as it should be. In the lower panels the quadrature results are compared to the various approximations obtained in the previous section.

In section 4.3 we compare rate and CV with simulation results of the Θ neuron using either the Stratonovich or Ito interpretation and compare the results to those of Gutkin and Ermentrout (1998). The effect of finite threshold and reset values is discussed in section 4.4.

4.1 Rate and CV as Functions of Noise Intensity. The rate depicted in Figure 3 behaves at large noise intensity rather independently of the value of β; it is seen to increase in proportion to $D^{1/3}$ according to equation 3.6. The effect of β becomes apparent at small noise intensity, where the rate (1) saturates if $\beta > 0$ at the value given by equation 3.9; (2) increases like $D^{1/3}$ for $\beta = 0$ according to equation 3.6; or (3) increases following an exponential dependence on inverse noise intensity (Kramers law, equation 3.10), for $\beta < 0$.

The approximation equation 3.10, for $\beta < 0$ (see Figure 3b, dashed line) is valid only for rather small noise intensity. In contrast, the result from linearization around $\beta = 0$ (see equation 3.11) fits pretty well for moderate to large noise intensity and for $\beta = 1$ or -1. In fact, one may interpolate between the weak and strong noise approximations without making an appreciable error.

The CV tends in the strong noise limit to $1/\sqrt{3}$, as predicted by equation 2.19. In the weak noise limit, it decreases either to zero ($\beta > 0$) corresponding to a perfectly regular firing for the oscillatory system in the absence of noise or tends to one ($\beta < 0$), indicating rare spiking with Poisson statistics. The exceptional case $\beta = 0$ leads to $CV = 1/\sqrt{3}$ for all noise intensities. Note that any finite value of β will lead to one of the other limits if the noise is sufficiently weak. Indeed for vanishing noise, $\beta = 0$ can be looked upon as a threshold value, as we will see.

[5] The sum formula equation 3.3 showed excellent agreement with the quadrature result, but is not discussed here.

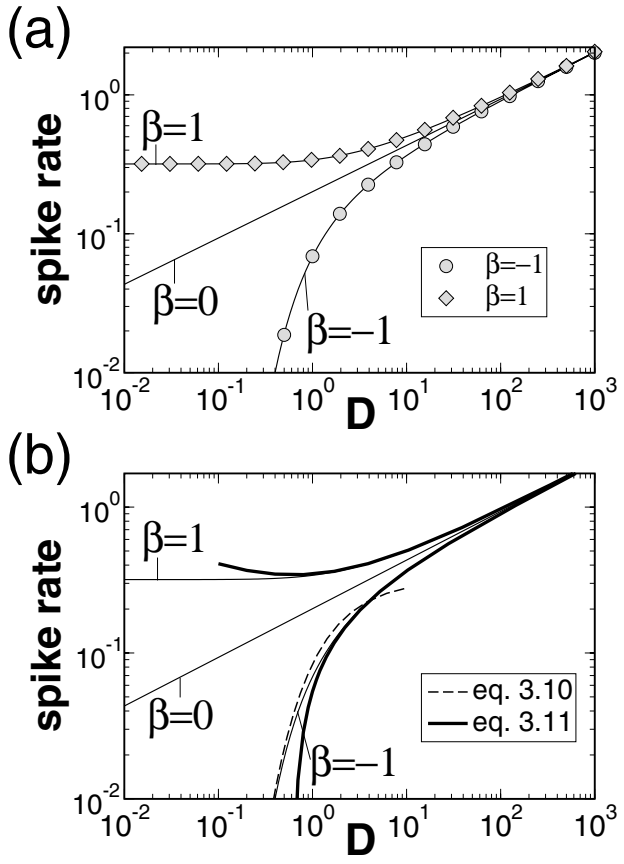

Figure 3: Spike rate of neuron versus noise intensity for the three distinct cases $\beta = \pm 1$ or 0 as indicated. (a) Quadrature results (thin lines) compared to simulations. (b) Quadrature results (thin lines) compared to Kramers rate (see equation 3.10, dashed line, only for $\beta = -1$), and linearization approximation (see equation 3.11, thick lines).

The approximation equation (3.9) is shown in Figure 4b as a dashed line. The "square-root" law (CV$\sim \sqrt{D}$) describes the true CV up to $D \approx 0.2$ rather well. For a general (positive) value of β, the approximation is valid for noise intensities that yield a CV below 0.25. This can be precisely formulated as a condition between D and β,

$$\beta > \left(\frac{12D}{\pi}\right)^{2/3}. \tag{4.1}$$

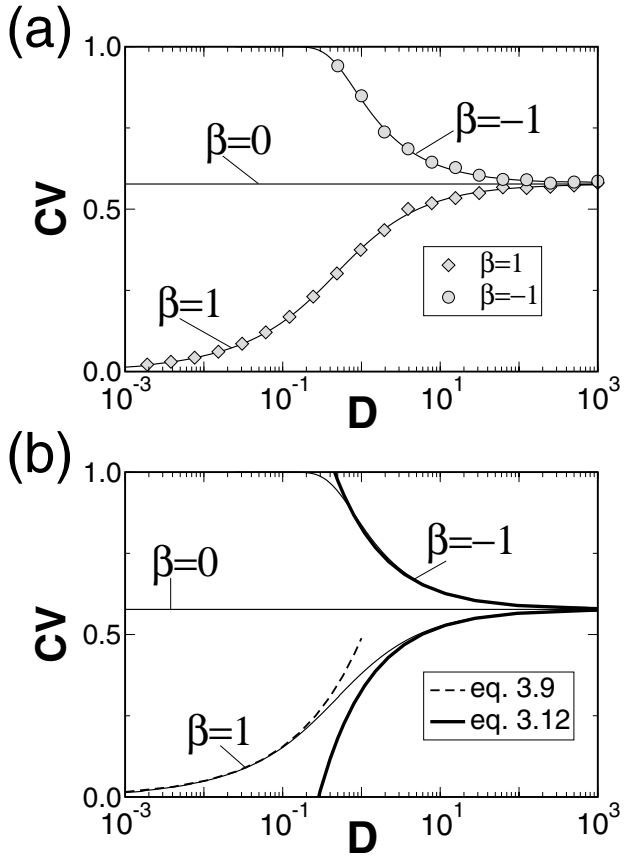

Figure 4: Coefficient of variation versus noise intensity for the three distinct cases $\beta = \pm 1$ or 0 as indicated. (a) Quadrature results compared to simulations. (b) Quadrature results compared to weak noise expansion (see equation 3.9, dashed line, only for $\beta = 1$), and linearization approximation (see equation 3.12, thick lines).

The linearization result shown by thick lines in Figure 4b seems to have an even larger range of validity. For $\beta = -1$, one may use the weak-input approximation equation (3.12) as a good estimate as long as the CV is below 0.9. For $\beta = 1$, the approximation coincides with the exact result in line thickness for CVs between 0.5 and $1/\sqrt{3}$. Via the scaling relation equation 2.18, these estimates can be generalized to arbitrary negative (positive) values of β, respectively since a change in input rescales only the noise intensity but not the range of CV.

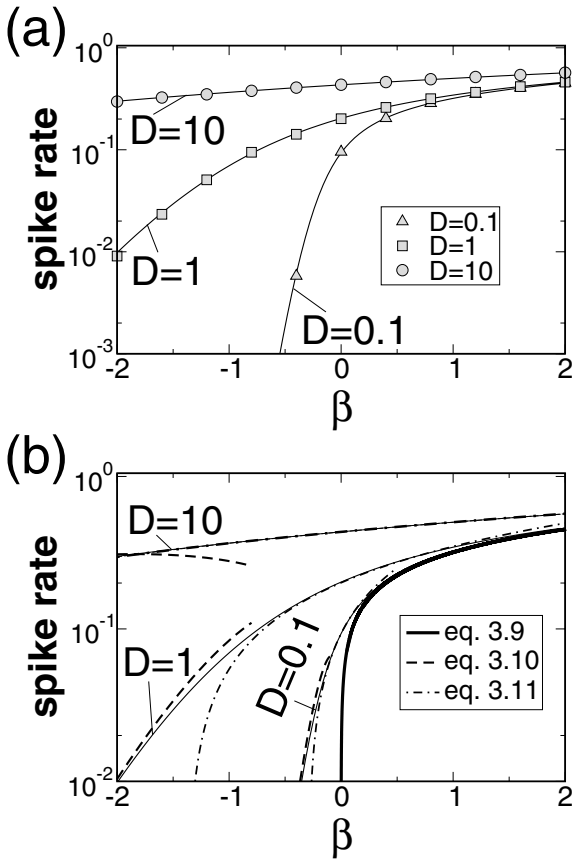

Figure 5: Spike rate of neuron versus input β for three different noise intensities as indicated. (a) Quadrature results compared to simulations. (b) Quadrature results compared to Kramers rate (see equation 3.10, dashed lines), linearization approximation (see equation 3.11, dashed-dotted lines), and the deterministic rate (see equation 3.9, thick line, only for $D = 0.1$).

4.2 Rate and CV as Functions of the Constant Input. Since β plays the role of an input, the dependencies of rate and CV on this parameter are of most interest. We show these dependencies for different noise intensities—$D = 0.1, 1$, or 10 in Figure 5 (rate) and Figure 6 (CV).

For strong noise, the dependence of the rate on input (see Figure 5) is rather weak. This can be readily understood: the linear part of the potential governed by β is of minor importance at large noise, and a potential barrier at negative β is "not seen." The passage through this region is biased diffusion (governed mainly by the cubic part of the potential that is independent of β).

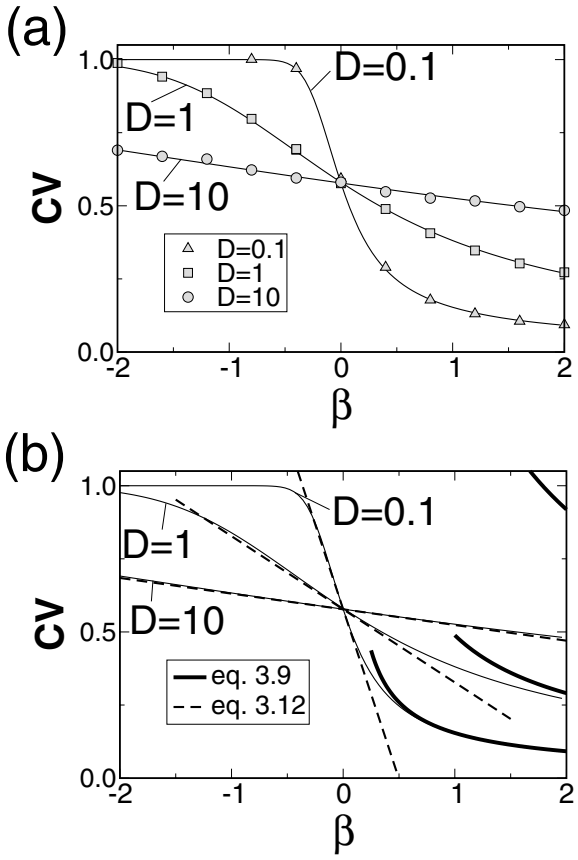

Figure 6: Coefficient of variation versus input β for three different noise intensities as indicated. (a) Quadrature results (thin lines) compared to simulations. (b) Quadrature results (thin lines) compared to weak noise expansion (equation 3.9, thick lines) and linearization approximation (equation 3.12, dashed lines). The latter coincides with the quadrature result almost within line thickness for $D = 10$.

Decreasing noise results in an increasing dependence of the rate on input, and for negative β, the rate can become arbitrary low. In the limit of vanishing noise, the rate can likewise attain arbitrary low values for positive input. This is one of the characteristic features of type I neurons (Ermentrout, 1996).

The approximation equation 3.10 is shown in Figure 5 by dashed lines. Although it well describes the data for $D = 0.1$, it becomes worse with increasing noise intensity over the range of β shown in Figure 6b. On the contrary, the linearization result agrees best at large noise intensity; indeed,

there is no visible difference between the quadrature result and the approximation for $D = 10$. At moderate noise intensity ($D = 1$), the linear behavior is restricted to a much smaller range of β. For small noise intensity and increasing β, the rate switches very fast from almost zero to a saturation value—a rather nonlinear behavior that is not well described (or only in a very small range around $\beta = 0$) by the linearization approximation equation 3.11.

The shape of the CV versus β curve is almost linear for strong noise (see Figure 6, lines for $D = 10$) as already mentioned by Gutkin and Ermentrout (1988). Since the quadrature formulas always contain β/D, a linearization of rate and CV with respect to β is valid for a larger range of β if D is large. Indeed, noise linearizes not only the transfer function (i.e., rate versus input parameter) but also all other statistical quantities with respect to variations of β. The linear dependence is, however, changed into a threshold-like dependence for small noise. With a look at the different small noise limits of the CV for $\beta < 0, \beta > 0$, no other behavior than this threshold behavior is indeed possible. The approximation according to equation 3.9 is shown by thin dashed lines in Figure 6. It can be used only for the small noise level $D = 0.1$ where the CV is below 0.25 and is far off for larger noise intensities.

4.3 Comparison to Simulations of the Θ Neuron Model. In section 2.2 we derived that the Stratonovich interpretation of the white-noise-driven Θ neuron model equation 2.8 is completely equivalent to our basic model, equation 2.1. That means that if we simulate using the scheme equation 2.9, we should exactly obtain the same rate and CV as for the original model. On the contrary, the Ito interpretation of equation 2.8 and the corresponding integration scheme equation 2.10 should result in different rate and CV, in particular, at larger noise intensity. Here we ask whether these differences are serious. We will compare also with results by Gutkin and Ermentrout (1998), who have apparently used the Ito scheme, equation 2.10, which does not exactly correspond to the original dynamics.

In Figure 7, the firing rate is shown as a function of the noise intensity for $\beta = \pm 1$ and $\beta = 0$. The quadrature result for the original dynamics equation 2.1 is compared to simulation results using the two integration schemes, equations 2.9 and 2.10. While the Stratonovich scheme exactly matches the analytical curves and thereby confirms our expectation, the rate obtained by simulating the Ito scheme is below the true rate for moderate to large noise intensities and saturates in the strong noise limit. Most remarkably, for $\beta = 1$, the rate does not depend on noise intensity at all, in marked contrast to the $D^{1/3}$ increase of the true rate for strong noise (in appendix B, we derive that the mean ISI, and hence the rate, do not depend on D for the specific input $\beta = 1$). As expected, both schemes yield the same function in the weak noise limit where the Stratonovich drift (proportional to noise intensity) becomes negligible.

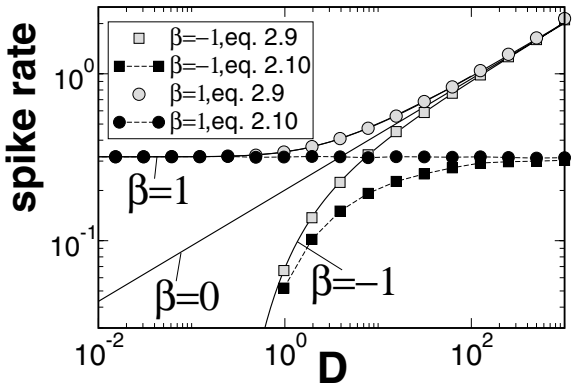

Figure 7: Firing rate as a function of noise intensity. Theory for the saddle-node system shown by solid lines for different values of β as indicated; simulation results for the Θ model in Stratonovich interpretation according to the integration scheme, equation 2.9, (gray symbols), and in Ito interpretation according to equation 2.10 (black symbols).

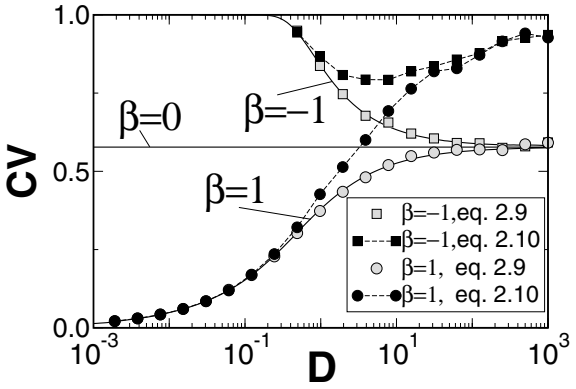

Figure 8: Coefficient of variation as a function of noise intensity. Theory for the saddle-node system shown by solid lines for different values of β as indicated; simulation results for the Θ model in Stratonovich interpretation according to the integration scheme, equation 2.9 (gray symbols) and in Ito interpretation according to equation 2.10 (black symbols).

Figure 8 shows the CV as a function of noise intensity for the three standard values of β. Here, the differences between the Ito and Stratonovich interpretations of the Θ neuron model are more important. The latter again yields perfect agreement with the theoretical result for the original dynamics. The Ito scheme, in contrast, shows strong deviations for moderate to

large noise intensity. The CV for the oscillatory regime ($\beta = 1$) is no longer restricted to $(0, 1/\sqrt{3})$. For both positive and negative β, the CV is always above the true CV.

Increasing noise even leads to a growth of the CV, such that for $\beta = -1$, a minimum in the CV versus noise intensity curve is seen. Such a minimum is a signature of coherence resonance (Pikovsky & Kurths, 1997). Many excitable (as opposed to periodically firing) systems exhibit their most regular spiking (as indicated by a minimal CV) if driven by a noise with finite "optimal" intensity. This effect is clearly absent for the original dynamics equation 2.1. This qualitative difference between the Ito and Stratonovich interpretations, in the form of the existence of such a minimum, might be irrelevant in real type I neurons since the reduction from the multidimensional system to the one-dimensional normal form becomes somewhat doubtful in the strong noise limit.

Gutkin and Ermentrout (1998) showed by means of numerical simulations that the Θ neuron exhibits (at least for $\beta < 0$) always a high CV, close to one. They started, as we did, with the normal form, derived the equation for the Θ neuron, but interpreted this equation apparently in Ito's sense (i.e., integrated equation 2.10). Although their conclusions are qualitatively correct, we would like to point out a quantitative discrepancy resulting from using the Ito scheme.

In Figure 6c of Gutkin and Ermentrout (1998) the CV is shown as a function of the mean interval, a representation of the data that is independent of the definition of noise intensity (they use a parameter σ that is related to the noise intensity D by $\sigma = \sqrt{2D}$). For a mean ISI ranging from 1 up to 10,000, they find a CV between 0.75 and 1.1 with a minimal CV at a small mean ISI (between 1 and 10). Data are pretty noisy, and Gutkin and Ermentrout (1998) do not mention the apparent minimum of the CV. We may use our data from Figures 7 and 8 and also plot a CV versus mean ISI curve; this is shown in Figure 9. Simulating the Ito version of the Θ model, we recover indeed a high CV and a minimum at a low mean interval.[6] In contrast, for the original model of a saddle-node system (theoretical curve, solid line in Figure 8) as well as for simulation results from the Θ model interpreted in Stratonovich's sense, we obtain no minimum in the CV and observe

[6] We note two discrepancies with the data of Gutkin and Ermentrout (1998): (1) We cannot plot a CV for an interval below $\langle T \rangle = 3.14$ since the rate is limited by the inverse of this value (cf. Figure 7), whereas in Gutkin and Ermentrout (1998), there is one data point for $\langle T \rangle = 1.5$. (2) The CV we have found in our simulation for $\beta = -1$ is always between 0.8 and 1, whereas in Gutkin and Ermentrout (1998), this range is slightly larger ($CV \in (0.75, 1.1)$). Either difference can be explained by insufficient statistics in Gutkin and Ermentrout (1998) and possibly (since there seems to be also a systematic deviation) by too large a time step in the integration procedure. Especially at low mean ISIs (high noise intensities), we had to use time steps down to $\Delta t = 10^{-4}$ to achieve independence of the data with regard to time step.

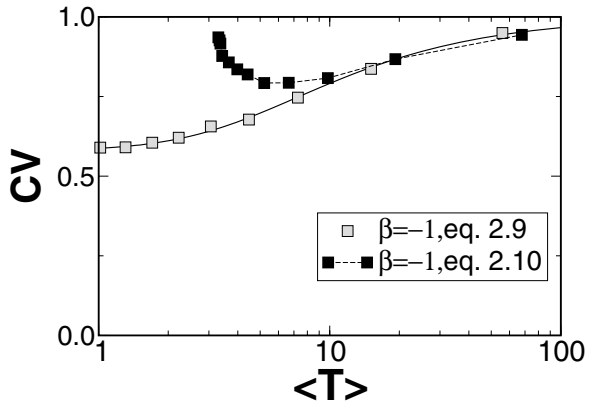

Figure 9: Coefficient of variation as a function of the mean ISI. Variation of the mean ISI is as in Gutkin and Ermentrout (1998), achieved by changing the noise intensity while keeping fixed $\beta = -1$. Theory for the saddle-node system shown by solid line; simulation results for the Θ model in Stratonovich interpretation according to the integration scheme equation 2.9 (gray) and in Ito interpretation according to equation 2.10 (black).

generally a considerably lower CV at small mean intervals. The lower limit is given by the large noise limit of the CV; in the excitable regime, we have $CV > 1/\sqrt{3}$. In the Stratonovich interpretation of the model as well as in the original dynamics, we can have arbitrary low mean interspike intervals, that is, arbitrary high firing rate.

4.4 Effect of Finite Threshold and Reset Values. As already mentioned, the spike generator model, 2.1, together with the reset rule, equation 2.3 has been used with finite threshold and reset values x_+ and x_-, respectively, in studies of neuronal networks (Latham et al., 2000; Hansel & Mato, 2001) (the spike generator was referred to as quadratic integrate-and-fire neuron model). This is also the case for our model simulations, as well as in our numerical evaluation of the quadrature formulas. So it is desirable to know how a finiteness of the boundaries[7] in the first passage problem influences rate and CV. This is an interesting problem on its own and will be studied in detail elsewhere.

In short, we can expect the following changes: (1) the scaling relations, equations 2.16 through 2.18, have to be modified (as they will now include rescaled values of x_+ and x_-); (2) significant changes to rate and CV are to

[7] Actually, only the threshold point is a boundary (absorbing barrier). The second boundary (reflecting barrier) is at $-\infty$, so the trajectory started at x_- is not prevented going toward $-\infty$.

be expected at large noise intensity; (3) as long as the (now finite) region of passage includes the fixed points of the system, rate and CV will be higher than for infinite boundaries. To understand the last prediction, it is useful to think of splitting the passage for the infinite boundaries into three passage problems: to go (1) from $-\infty$ to a finite value x_-, (2) from x_- to x_+, and (3) from x_+ to ∞. Since we are dealing with a Markov process, these passages and the moments of their durations are statistically independent. Now, considering a system with finite boundaries amounts to neglecting the outside passages 1 and 3. From this picture, it becomes clear that the mean passage time will be shorter than for infinite boundaries. Furthermore, the passages on the outside are governed by strong forces (recall the square term in equation 2.1) and are therefore more regular than the passage through the "inside" region (i.e., the CV of the passage times for the outside region is expected to be lower than for the passage from x_- to x_+). It can be readily shown that this implies a higher variability of the passage time (or ISI) for the case where the outside passages are not taken into account.

In Figure 10, we show how rate and CV versus noise intensity change for different values of β if we choose $x_\pm = \pm 2$ (this is a rather drastic reduction of the reset-threshold distance). These curves were obtained using the general formula, equations A.1 and A.4 from appendix A, together with the potential equation, 2.6. We compare the modified rate and CV (thick lines) to the old results for infinite $x_\pm$ (thin lines).

The rate (see Figure 10a) is generally larger for finite $x_\pm$ as expected. At small noise, the differences with the infinite boundary case are minor. For $D \to 0$, the rate converges to that with infinite boundaries if $\beta \leq 0$. However, for $\beta = 1$, we see in the small noise limit a difference between the deterministic rates $\sqrt{\beta}/\pi$ and $\sqrt{\beta}[\pi - (\arctan(x_+/\sqrt{\beta}) - \arctan(x_-/\sqrt{\beta})]^{-1}$ for the cases of infinite and finite threshold and reset points, respectively. Further, for all β, the deviations are more serious at large noise intensity. The rate grows for the finite case in proportion to $D^{2/3}$ (not like $D^{1/3}$ as for the case of infinite boundaries). This can be understood by the large-D asymptotics of the integrals in equation A.1.

The CV shows also a drastic qualitative change in its shape. Generally, it converges to the CV for infinite boundaries in the low noise limit, but grows unbounded in the large D limit, in marked contrast to the model with infinite $x_\pm$. This growth goes as $D^{1/6}$ as can be again concluded from the asymptotics of the integrals in equations A.1 and A.4. We would like to point out that this holds for all values of β; even for $\beta = 0$, where we had remarkably a constant CV in the case of infinite boundaries, the CV does increase with increasing noise intensity like $D^{1/6}$. Most notably, a minimum in the CV is observed for $\beta = -1$ (coherence resonance; cf. the discussion in the previous section). Thus, the absence of coherence resonance (i.e., an finite "optimal" noise intensity) was a consequence of using infinite boundaries.

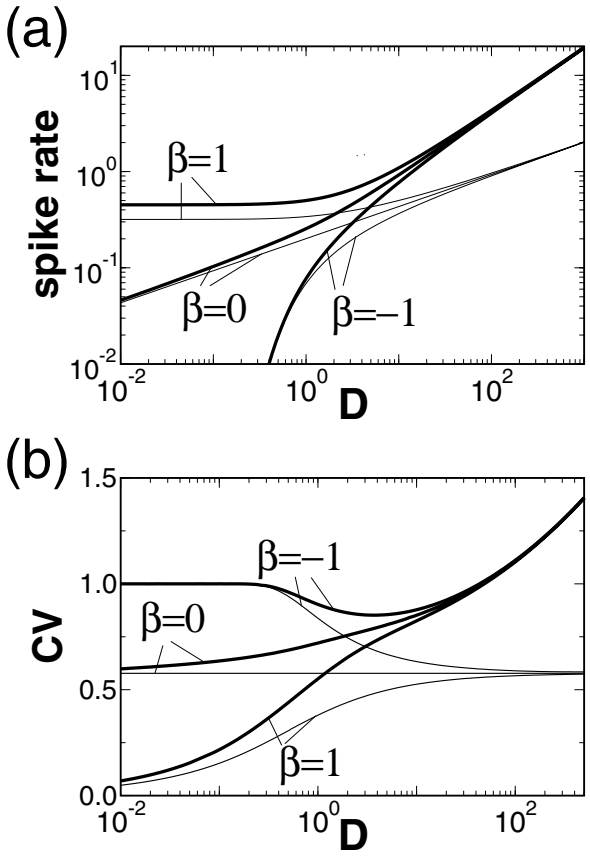

Figure 10: Spike rate of (a) neuron and (b) coefficient of variation versus noise intensity for three values of β as indicated. Thin lines are quadrature results as shown before in Figure 3 and Figure 4; thick lines are quadrature results for finite threshold and reset values, $x_- = -2$ and $x_+ = 2$, respectively.

In general, rate and CV for the finite and infinite cases agree best for negative β and small noise intensity. Increasing the modulus of threshold and reset points will improve the agreement, in particular, for small to moderate noise. This means plotting rate or CV for $x_\pm = \pm 10$ and a particular value of β, curves will be obtained that are in between those for $x_\pm = \pm 2$ and $x_\pm = \pm\infty$.

From a computational point of view, large values of $x_\pm$ increase the simulation time. An estimate of the computation time saved by using $x_\pm = \pm 2$ instead of $x_\pm = \pm 500$ (i.e., infinite values for practical purposes) can be inferred from the distance between the spike rates for either case in Figure 10;

at very strong noise, this is about one order of magnitude, whereas at small to moderate noise intensity, the difference in computation time appears to be negligible.[8]

Another question is which kind of threshold and reset conditions is suitable with respect to more realistic type I neuron models and, of course, real type I neurons. This important issue is currently under investigation.

5 Discussion and Conclusions

We have considered a simple spike generator model that involves the one-dimensional normal form of a saddle-node bifurcation and may be used to represent a type I neuron. The model seems to be computationally simpler than the equivalent Θ neuron often used in neurocomputational research. Using the spike generator with saddle-node bifurcation helps, moreover, to avoid the pitfalls associated with using multiplicative white noise as in the Θ model.

A second advantage of the saddle-node spike generator is that we were able to adopt many useful analytic results for the passage time problem from the statistical physics literature on a related problem. We discussed the remarkable scaling behavior of the model, which allows reducing the number of parameters in the problem. We gave the exact quadrature expressions for mean and variance of the ISI and a simple sum formula for the mean ISI. Furthermore, we derived expressions for simple limiting cases for rate and CV of the model. All results may be useful also for problems involving networks of type I neurons.

For the problem of high variability of spike trains of cortical neurons, one of our conclusions is especially relevant: given a negative input ($\beta < 0$), the CV is restricted to the interval $(1/\sqrt{3}, 1)$. It can never be lower than the high noise limit CV of the model. This stands in marked contrast to the leaky integrate-and-fire model, which can in this regime attain arbitrary low values of the CV if the input parameter is tuned to a certain small negative value and can be as well arbitrary high for both sub- and suprathreshold input (Lindner, 2002; Lindner, Schimansky-Geier, & Longtin, 2002). Although Gutkin and Ermentrout (1998) overestimated the CV with their simulation results, their main conclusion remains valid: type I neurons stimulated by white gaussian noise show a high variability for arbitrary but negative input. Future work will consider a comparison of our results with a two-(or higher-) dimensional dynamics of an ionic model of a type I neuron, such as Morris-Lecar. We will also consider the theoretical analysis of the phase resetting curves and the response of the stochastic saddle-node neuron model studied here to periodic and broadband input.

[8] Larger modulus of $x_\pm$ requires also a smaller time step (or an adaptive time step), which will increase the computation time.

Appendix A: Derivation of the Quadrature Formulas

The classical formulas for the first two moments of the first passage time in an arbitrary potential $V(x)$ from x_- to x_+ with reflecting boundary at $-\infty$ were given by Pontryagin et al. (1933) (for a more recent reference, see Anishchenko, Astakhov, Neiman, Vadivasova, & Schimansky-Geier, 2002, chapter 1.2, equation 1.248)

$$\langle T(x_- \to x_+)\rangle = \frac{1}{D}\int_{x_-}^{x_+} dx\, e^{V(x)/D} \int_{-\infty}^{x} dy\, e^{-V(y)/D}, \tag{A.1}$$

$$\langle T^2(x_- \to x_+)\rangle = \frac{2}{D^2}\int_{x_-}^{x_+} dx\, e^{V(x)/D} \int_{-\infty}^{x} dy\, e^{-V(y)/D} \times \int_{y}^{x_+} du\, e^{V(u)/D} \int_{-\infty}^{u} dv\, e^{-V(v)/D}. \tag{A.2}$$

The resulting expression for the variance $\langle \Delta T^2\rangle = \langle T^2\rangle - \langle T\rangle^2$ can be simplified by interchanging several times the integration boundaries and the names of the variables (see, e.g., in Sigeti, 1988, chap. 4, for the potential equation 2.6 with $\beta = 0$ or in Reimann et al., 2002, for the case of a periodic potential), yielding

$$\langle \Delta T^2\rangle = \frac{2}{D^2}\int_{x_-}^{x_+} dx\, e^{V(x)/D} \int_{-\infty}^{x} dz\, e^{-V(z)/D} \left[\int_{-\infty}^{z} dy\, e^{-V(y)/D}\right]^2. \tag{A.3}$$

Another interchange of variables leads to (Lindner, 2002)

$$\langle \Delta T^2\rangle = \frac{2}{D^2}\int_{-\infty}^{x_+} dz\, e^{V(z)/D} \left[\int_{-\infty}^{z} dy\, e^{-V(y)/D}\right]^2 \times \int_{z}^{x_+} dx\, \Theta(x - x_-) e^{V(x)/D}, \tag{A.4}$$

(here, $\Theta(x)$ is Heaviside's step function), a formula that is much easier to evaluate numerically than the original expressions.

Inserting the potential equation 2.6 into equations A.1 and A.4 with $x_\pm = \pm\infty$ and using new integration variables like $\tilde{x} = x/\sqrt[3]{3D}$, we obtain equations 3.1 and 3.2.

Appendix B: Mean First Passage Time of the Θ Neuron in the Ito Interpretation

In section 4.3 we have seen from the simulation results that the rate of the Θ neuron model interpreted in the sense of Ito does not depend on D if $\beta = 1$. Although irrelevant for the saddle-node system (correctly, we have to use the Stratonovich interpretation of the Θ model), this is a remarkable finding, which is analytically proven in the following. The Ito scheme, equation 2.10, corresponds to the following stochastic differential equation interpreted in the Stratonovich sense:

$$\dot{\Theta} = 1 - \cos(\Theta) + (\beta + D\sin(\Theta)) \times (1 + \cos(\Theta)) + \sqrt{2D}(1 + \cos(\Theta))\xi(t). \tag{B.1}$$

Here, the additional term $+D\sin(\Theta)$ compensates the Stratonovich drift $-D\sin(\Theta)$ in the Stratonovich integration scheme, equation 2.9, and hence this scheme leads now to what was before the Ito scheme, equation 2.10. Since we use the Stratonovich interpretation, we can transform equation B.1 back to the old variable $x(t)$ by means of equation 2.7, yielding

$$\dot{x} = \beta + x^2 + \frac{2Dx}{1+x^2} + \sqrt{2D}\xi(t). \tag{B.2}$$

Hence, interpreting the Θ neuron model with white noise in the Ito sense amounts to the introduction of a noise-dependent modification in the potential V(x) given by equation 2.6. The modified potential reads

$$\tilde{V}(x) = -\frac{x}{3} - \beta x - D\ln(1 + x^2). \tag{B.3}$$

Inserting this into the general formula for the mean first passage time yields

$$\langle T\rangle = \frac{1}{D}\int_{-\infty}^{\infty} dx\, \frac{\exp[-(x^3/3 + \beta x)/D]}{1+x^2} \times \int_{-\infty}^{x} dy\, (1+y^2)\exp[(y^3/3 + \beta y)/D], \tag{B.4}$$

which for $\beta = 1$ can be simplified:

$$\langle T\rangle = \frac{1}{D}\int_{-\infty}^{\infty} dx\, \frac{\exp[-(x^3/3 + x)/D]}{1+x^2} \int_{-\infty}^{x} dy\, D\frac{d}{dy}(\exp[(y^3/3 + y)/D]),$$

$$= \int_{-\infty}^{\infty} dx \frac{1}{1+x^2} = \pi. \tag{B.5}$$

Hence the rate is exactly given by

$$r = 1/\pi, \tag{B.6}$$

as it was also found in the simulations within the numerical accuracy. Note that for any value $\beta \neq 1$, the rate is expected to depend on D.

Acknowledgments

This research was supported by NSERC Canada and a Premiers Research Excellence Award (PREA) from the Government of Ontario. We also thank Christophe Langevin for preliminary numerical calculations of first passage times in the Θ neuron model and Jan Benda for a careful reading of the manuscript.

References

Abramowitz, M., & Stegun, I. A. (1970). *Handbook of mathematical functions*. New York: Dover.

Anishchenko, V. S., Astakhov, V. V., Neiman, A. B., Vadivasova, T. E., & Schimansky-Geier, L. (2002). *Nonlinear dynamics of chaotic and stochastic systems*. Berlin: Springer-Verlag.

Arecchi, F. T., & Politi, A. (1980). Transient fluctuations in the decay of an unstable state. *Phys. Rev. Lett., 45*, 1219.

Bell, A., Mainen, Z., Tsodyks, M., & Sejnowski, T. (1995). *"Balancing" of conductances may explain irregular cortical spiking* (Tech. Rep. INC-9502). San Diego: Institute for Neural Computation, University of California, San Diego.

Bulsara, A., Lowen S. B., & Rees, C. D. (1994). Cooperative behavior in the periodically modulated Wiener process: Noise-induced complexity in a model neuron. *Phys. Rev. E, 49*, 4989.

Colet, P., San Miguel, M., Casademunt, J., & Sancho, J. M. (1989). Relaxation from a marginal state in optical bistability. *Phys. Rev. A, 39*, 149.

Cox, D. R. (1962). *Renewal theory*. London: Methuen.

Ermentrout, G. B. (1996). Type I membranes, phase resetting curves, and synchrony. *Neural Comp., 8*, 979.

Gang, H., Ditzinger, T., Ning, C. Z., & Haken, H. (1993). Stochastic resonance without external periodic force. *Phys. Rev. Lett., 71*, 807.

Gardiner, C. W. (1985). *Handbook of stochastic methods*. Berlin: Springer-Verlag.

Gutkin, B. S., & Ermentrout, G. B. (1998). Dynamics of membrane excitability determine interspike interval variability: A link between spike generation mechanisms and cortical spike train statistics. *Neural Comp., 10*, 1047.

Hansel, D., & Mato, G. (2001). Existence and stability of persistent states in large neuronal networks. *Phys. Rev. Lett., 86*, 4175.

Hodgkin, A. (1948). The local electric changes associated with repetitive action in a medullated axon. *J. Physiol., 107*, 165.

Hoppensteadt, F. C., & Izhikevich, E. M. (1997). *Weakly connected neural networks*. New York: Springer-Verlag.

Kramers, H. A. (1940). Brownian motion in a field of force and the diffusion model of chemical reactions. *Physica, 7*, 284.

Latham, P. E., Richmond, B. J., Nelson, P. G., & Nirenberg, S. (2000). Intrinsic dynamics in neuronal networks. I. Theory. *J. Neurophysiol., 83*, 808.

Lindner, B. (2002). *Coherence and stochastic resonance in nonlinear dynamical systems*. Berlin: Logos-Verlag.

Lindner, B., Schimansky-Geier, L., & Longtin, A. (2002). Maximizing spike train coherence or incoherence in the leaky integrate-and-fire model. *Phys. Rev. E, 66*, 031916.

Longtin, A. (1997). Autonomous stochastic resonance in bursting neurons. *Phys. Rev. E, 55*, 868.

Morris, C., & Lecar, H. (1981). Voltage oscillations in the barnacle giant muscle fiber. *Biophys. J., 35*, 193.

Pikovsky, A., & Kurths, J. (1997). Coherence resonance in a noise-driven excitable system. *Phys. Rev. Lett., 78*, 775.

Pontryagin, L., Andronov, A., & Witt, A. (1989). On the statistical treatment of dynamical systems. In F. Moss & P. V. E. McClintock (Eds.), *Noise in nonlinear dynamical systems* (Vol. 1, p. 329). Cambridge: Cambridge University Press.

Rappel, W. J., & Strogatz, S. H. (1994). Stochastic resonance in an autonomous system with a nonuniform limit cycle. *Phys. Rev. E, 50*, 3249.

Reimann, P., Van den Broeck, C., Hänggi, P., Linke, H., Rubi, J. M., & Pérez-Madrid, A. (2002). Diffusion in tilted periodic potentials: Enhancement, universality, and scaling. *Phys. Rev. E, 65*, 031104.

Rinzel, J., & B. Ermentrout, B. (1989). Analysis of neural excitability and oscillations. In C. Koch & I. Segev (Eds.), *Methods in neuronal modeling* (p. 251). Cambridge, MA: MIT Press.

Risken, H. (1984). *The Fokker-Planck equation*. Berlin: Springer-Verlag.

Shadlen, M. N., & Newsome, W. T. (1994). Noise, neural codes, and cortical organization. *Curr. Op. Neurobiol., 4*, 569.

Sigeti, D. (1988). *Universal results for the effects of noise on dynamical systems*. Unpublished doctoral dissertation, University of Texas at Austin.

Sigeti, D., & Horsthemke, W. (1989). Pseudo-regular oscillations induced by external noise. *J. Stat. Phys., 54*, 1217.

Softky, W. R., & Koch, C. (1993). The highly irregular firing of cortical cells is inconsistent with temporal integration of random EPSPs. *J. Neuronsci., 13*, 334.

Troyer, T., & Miller, K. (1997). Physiological gain leads to high ISI variability in a simple model of a cortical regular spiking cell. *Neur. Comp., 9*, 971.

Tuckwell, H. C. (1988). *Introduction to theoretical neurobiology*. Cambridge: Cambridge University Press.

Wilbur, W., & Rinzel, J. (1983). A theoretical basis for large coefficient of variation and bimodality in neuronal interspike interval distributions. *J. Theor. Biol., 105*, 345.

Received October 31, 2002; accepted February 4, 2003.